UTILIZING WAVELET TRANSFORM FOR ML RECONSTRUCTION IN POSITRON EMISSION TOMOGRAPHY

Pavel Kisilev, Matthew Jacobson, Yehoshua Y. Zeevi

Dept. of Electrical Engineering
Technion, Israel Institute of Technology, Haifa, 32000, Israel

Abstract – **A classical technique for reconstruction of Positron Emission Tomography (PET) images from measured projections is based on the maximum likelihood (ML) parameter estimation combined with the Expectation Maximization (EM) algorithm. We incorporate the Wavelet transform (WT) into the ML framework, and obtain new iterative algorithms that incorporate local and multiresolution properties of the WT within the structure of the EM algorithm and the recently proposed conjugate barrier (CB) algorithm. Using the WT allows one to embed regularization procedures (filtering) into the iterative process, by imposing a subset of wavelet coefficients with a desired resolution on the objective function. Properties of the proposed algorithm are demonstrated on reconstructions of a synthetic brain phantom, and the quality of reconstruction is compared with standard methods.**

Keywords – **medical imaging, positron emission tomography, expectation maximization, wavelets**

1. INTRODUCTION

PET is a medical imaging technique that enables one to quantify a distribution of radioactivity within the body, and, as such, it is useful in detection and identification of pathological tissue. In this technique, radioactive tracers, injected into the body of a patient, emit photons, which are detected in distinct detector pairs, or bins. By counting the number of photons detected in the various bins, one measures the projection of the tracer distribution at different angles. A classical technique for the reconstruction of 2D and 3D PET images from measured projections is based on the maximum likelihood (ML) framework [1]. Utilizing particular properties of the Poisson process leads to the Expectation Maximization (EM) algorithm for PET reconstruction [2]. This algorithm provides reliable reconstruction results with high resolution. However, it does not exploit the localized nature of images, nor their multiresolution structure.

Furthermore, reconstruction of images from their projections usually requires some kind of regularization that represents a trade-off between accuracy and resolution. Image reconstruction using so-called blobs functions was discussed in [3] and [4]. It allows one to control the smoothness properties of the reconstructed image by choosing appropriately the value of the smoothness parameter of the blobs functions.

Applying the Wavelet transform (WT) to the image entails a change of the parameter space and leads to a new iterative algorithm that incorporates local and multiresolution properties of the WT within the structure of the EM algorithm. Another alternative for utilizing the WT is to use penalty function defined in the wavelet domain.

The desired regularization can be accomplished in a natural way in both cases; using the WT allows one to embed regularisation procedures (filtering) into the iterative process, as compared with conventional post-filtering. This task is accomplished by imposing a new set of parameters on a subset of wavelet coefficients corresponding to desired resolutions.

We first describe the basics of the PET image reconstruction technique based on the ML framework. Next, we present the wavelet-based ML reconstruction techniques for PET reconstruction, and consider some computational issues. Finally, we discuss the advantages of the proposed methods and illustrate their potential by a simulation study.

2. ML RECONSTRUCTION OF PET IMAGES

EM algorithm

We first summarize some of the main results of L. Shepp and Y. Vardy [2] who pioneered the ML image reconstruction in PET by application of the EM algorithm.

Let the total number of photons detected in each bin be $y(b)$, $b = 1,\ldots,B$. Let the body be divided into voxels (or pixels), and the number of photons generated independently within each voxel be $n(v)$, $v = 1,\ldots,V$. Generation of photons in each voxel is described by the Poisson process, characterized by the expected value of photons $\lambda(v)$:

$$f(n|\lambda(v)) = P(n(v) = n|\lambda(v)) = e^{-\lambda(v)} \frac{\lambda(v)^n}{n!} \quad (1)$$

The values $\lambda(v)$ depend on the tracer distribution, which, in turn, depend on the tissue structure in the body. In addition, variables $y(b)$ are independent and Poissonian with expected values $\lambda(b)$:

$$f(y|\lambda(b)) = P(y(b) = y|\lambda(b)) = e^{-\lambda(v)} \frac{\lambda(b)^y}{y!} \quad \textbf{(2)}$$

Let $p(v,b)$ denote the probability of the event that a photon emitted from voxel v is detected in bin b, forming a matrix with VxB entries. The probability matrix values depend on various physical factors such as scanner geometry, detector efficiency, and the composition of the body being scanned. The issue of computing $p(v,b)$ will be discussed later.

From (2) the log-likelihood function for the measurements $y(b)$ is given by

$$L(\lambda) = \sum_v \lambda(v)p(v) + \sum_b y(b)\log\sum_v \lambda(v)p(v,b), \quad (3)$$

where $\lambda = \{\lambda(v),\ v = 1,\ldots,V\}$ is the set of unknown parameters, and

$$p(v) = \sum p(v,b) \quad (4)$$

is the so-called sensitivity image (i.e. the probability that an emission from v is detected).

To solve (3), the EM algorithm was applied to the PET reconstruction problem leading to the following formula

$$\lambda^{(k+1)}(v) = \frac{\lambda^{(k)}(v)}{p(v)} \sum_{b=1}^{B} \frac{y(b)p(v,b)}{\sum_{v'=1}^{V} \lambda^{(k)}(v')p(v',b)}, \quad \forall v \quad (5)$$

for iteratively approximating a maximizer of $L(\boldsymbol{\lambda})$.

Conjugate Barrier (CB) algorithm

The CB algorithm proposed lately in [5] is a kind of a version of the standard Gradient Descent algorithm.

Let the function h be defined as:

$$h(x)=\begin{cases}\| x \|_p, & x\in\Delta\\ +\infty, & x\notin\Delta,\end{cases}$$

where $\|\cdot\|_p$ denotes the l_p norm, and Δ is the domain of valid values of x. In our setting, wherein x is the value of normalized image intensity

$$\Delta \equiv \{x\in R^n \mid x\geq 0, \sum_1^V x(v)=1\}.$$

Let h_* be the so-called conjugate function of h, and

$$h_*(\xi)=\sup_{x\in\Delta}[\xi^T x-h(x)],$$

where ξ is the conjugate image, so that $\xi,\lambda\in R^V$. The initial value ξ^0 can be initialized arbitrary The following two iterative steps summarizes the CB algorithm:

step 1: $\lambda^{n+1}=\nabla h(\xi^{n+1})$

step 2: $\xi^{n+1}=\xi^n-\gamma^n\nabla L_{(p)}(\lambda^n),$

where $L_{(p)}(\lambda^n)$ is a (penalized) Log-likelihood function, γ^n is a positive step size.

The value of h_* at a given point ξ is found by solving the following optimization problem

$$\min_{x\in\Delta}[\xi^T x-\| x \|],$$

so that $h_*(\xi)$ is given as the optimal value of this problem, and $\nabla h_*(\xi)$ as the optimal solution. For more details see [5] and [6].

The CB algorithm has several advantages over the EM [7]: 1) its ordered sets version always converges 2) the rate of convergence is known and independent of the dimension of the problem, 3) the error bound is about $\sqrt{\log V}$. In addition, its computational cost is comparable to the EM.

We proceed to show two strategies of how to exploit wavelet representation in PET reconstruction.

3. WAVELET DOMAIN ML RECONSTRUCTION

The first strategy is applying the WT to the image, which results in a natural modification of the ML reconstruction scheme.

Let $\{\varphi_m\}$, $m=1,\dots,M$, where φ_m is an orthonormal wavelet basis vector of an M-dimensional vector space, and let the discrete image $\lambda(v)$, belonging to this vector space, be represented by this basis as follows:

$$\lambda(v) = \sum_{m=1} a_m \varphi_m(v) \qquad (6)$$
$$\lambda = \Phi a,$$

where

$$a_m = \sum_{v=1}^{V} \lambda(v)\varphi_m^*(v), \qquad (7)$$
$$a = \Phi^T \lambda.$$

(see more detailed discussion of the wavelet transform in the Appendix)

Then, estimating the true λ from data y is equivalent to estimating a from y, since $\hat{\lambda}_{ML}(y) = \Phi \hat{a}_{ML}(y)$ and $\hat{a}_{ML}(y) = \Phi^T \hat{\lambda}_{ML}(y)$. (We actually use here the invariance property of the ML estimate).

In particular, by substituting (6) into (3) we can transform the log-likelihood function as follows:

$$\begin{aligned} L(\lambda) &= \sum_v \sum_b \lambda(v) p(v,b) + \\ &+ \sum_b y(b) \log \sum_v \lambda(v) p(v,b) \\ &= \sum_v \sum_b \sum_m a(m) \varphi_m(v) p(v,b) + \\ &+ \sum_b y(b) \log \sum_v \sum_m a(m) \varphi_m(v) p(v,b), \end{aligned} \qquad (8)$$

and

$$\begin{aligned} L(\lambda) &= \sum_m a(m) \tilde{p}(m,b) + \\ &+ \sum_b y(b) \log \sum_m a(m) \tilde{p}(m,b), \end{aligned} \qquad (9)$$

where

$$\tilde{p}(m,b) = \sum_{v=1}^{V} p(v,b) \varphi_m(v) \qquad (10)$$

and

$$\tilde{p}(m) = \sum_{v=1}^{V} p(v) \varphi_m(v). \qquad (11)$$

Several known optimization techniques can be applied to solve Equation (9). The form of the transformed function in (9) is analogous to the original, which implies that the optimal $a(m)$ coefficients can be obtained via the wavelet domain iterative formula

$$a_l^{(k+1)} = a_l^{(k)} \frac{1}{\tilde{p}(l)} \sum_{b=1}^{B} \frac{y(b)\tilde{p}(l,b)}{\sum_{m \in U} a_m^{(k)} \tilde{p}(m,b)}, \qquad (12)$$

$$\forall l \in U,$$

while adding positive constraints on the resulting image values.

The wavelet domain raytracing procedure

Various techniques have been proposed for calculating the probability matrix, whose element are $p(v,b)$, in the original pixel (voxel) domain. In the context of the iterative schemes, there are two approaches: 1) to calculate this matrix in advance and store it, and 2) to calculate it on the fly. The size of the matrix tends to be very large for modern scanners making the first approach practical only for 2D reconstructions. The second approach may be implemented efficiently by computing only the $p(v,b)$ which are non-zero for a given b [2]. In an NxNxN image, the number of voxels that contribute to a certain bin b is $O(N)$.

One procedure which exploits this efficiency, the so-called ray tracing procedure, is usually used in practice. It was argued in [2] that the probability of an event, where emission in voxel v is detected in bin b, can be approximated by the length of intersection of the central line of response (LOR) of bin b with voxel v. The ray tracing procedure determines the coordinates of the voxels intersected by the central LOR and the corresponding intersection lengths.

The forward projection (FP) operation in the image domain in the context of PET is

$$y(b) = \sum_{v=1} \lambda(v) p(v,b). \qquad (13)$$

In this case, the basis for image representation consists of box functions, and the value of image intensity is uniform over each basis function, i.e. over each voxel. In contrast, the FP operation in the wavelet domain is

$$y(b) = \sum_{m \in U} a_m \tilde{p}(m,b) \qquad (14)$$

and we have to calculate the probability $\tilde{p}(m,b)$ that a particular wavelet function φ_m contributes to the value of $y(b)$. Now, the entry $\tilde{p}(m,b)$ of the probability matrix can be approximated by the X-ray transform of the wavelet function along the intersection of the central LOR of bin b with the support of this wavelet function. In the sequel we show how to calculate which wavelet functions contribute to a particular bin. Let the support of the 1D mother wavelet function be defined by its left and right coordinates as $\Delta(\varphi) := [x_l, x_r]$. Then, the support of the wavelet function with the scale and translation parameters s and t, respectively, is

$$\Delta(\varphi_{s,t}) = \left[s(x_l + t), s(x_r + t)\right]. \tag{15}$$

Therefore, for a 2D or 3D wavelet function with the scale parameter a to contribute to the position with the coordinates x,y,z, the corresponding translation parameters t_x, t_y, t_z must satisfy the following condition:

$$\frac{i}{s} - i_r \le t_i \le \frac{i}{s} - i_l, \quad \text{where } i = x, y, z \tag{16}$$

Since, due to the compressing property of the wavelet transform, there are only relatively few non-zero coefficients a_m, and a corresponding number of wavelet basis functions to be forward projected in order to calculate the relevant $\tilde{p}(m,b)$ entries on the fly. Nevertheless, the wavelet domain raytracing procedure is computationally demanding. In the next section we show how to achieve similar to the wavelet domain EM flexibility by applying wavelet domain penalties while working in the original image domain.

4. PENALIZED ML RECONSTRUCTION USING WAVELETS

As was mentioned before, natural PET data are usually very noisy due to a short acquisition time and various scatter effects. Minimizing the log-likelihood function of such (*apriori*) noisy data leads to a very noisy reconstructed image. In such cases, various penalty functions reflecting smoothness of the noise-free image or other prior information are used in order to improve quality of reconstruction. In this case, penalized log-likelihood function takes the form

$$L_p(\lambda) = L(\lambda) + \mu \mathrm{H}(\lambda) \tag{17}$$

where $\mathbf{H}(\lambda)$ is a penalty function and μ is the weight parameter.

The corresponding iterative formula for the penalized EM algorithm is

$$\lambda^{(k+1)}(v) = \frac{\lambda^{(k)}(v)}{p(v) + \mu\nabla\mathrm{H}(\lambda)} \sum_{b=1}^{B} \frac{y(b)p(v,b)}{\sum_{v'=1}^{V} \lambda^{(k)}(v')p(v',b)}, \quad \forall v, \tag{18}$$

where ∇ denotes gradient operator.

Utilizing the wavelet domain penalty

Several penalty functions were proposed in literature (e.g [8], [9]). These are usually applied to the original image domain. In this work we propose a new method that utilizes penalty functions defined in the wavelet domain.

Suppose, that for a particular WT $\boldsymbol{\Phi}$ a subset of coefficients of the image λ is of interest or, alternatively, that it is known that only a (small) number of coefficients which compose the subset are nonzero. In particular, let matrix $\boldsymbol{a}$ of the wavelet transform coefficients of the image can be partitioned as $\boldsymbol{a} = [\boldsymbol{b}\ \boldsymbol{c}]$, where $\boldsymbol{b}$ and $\boldsymbol{c}$ are so-called signal and noise subspaces, respectively, and $\boldsymbol{b}$ is the subset of interest.

This assumption represents sort of prior knowledge about the emission means λ, e.g. knowledge about a particular organ's metabolism, which defines in turn smoothness, presence of edges and other characteristics of the image λ. Therefore, such a parametric model based on the WT can be easily incorporated into the Bayesian reconstruction approach.

The original ML reconstruction problem with the above prior is formulated as:

$$\begin{cases} \max\limits_{\lambda}\{L(\lambda)\} \\ s.t.:\ (1)\,\lambda \geq 0 \\ \qquad\ \ (2)\,\boldsymbol{c}(\lambda) = 0 \end{cases}$$

This problem is not feasible since it is very difficult to satisfy both requirements simultaneously. Therefore, we formulate a penalized ML reconstruction problem as follows:

$$\begin{cases} \min\limits_{\lambda}\{-L(\lambda) + \mu\|\boldsymbol{c}(\lambda)\|_p\} \\ \text{s.t.: } \lambda \geq 0, \end{cases}$$

so that the penalty term is $\mathrm{H}(\lambda) = \|\boldsymbol{c}(\lambda)\|_p$. (We used the l_2 norm in our experiments).

In order to suppress high resolution noise while preserving edges we choose subset $\boldsymbol{c}$ to be constructed from the coefficients at the two highest resolutions.

5. EXPERIMENTAL RESULTS

We carried out tests with the Shepp-Logan phantom (Figure 1); a model used in tomography for evaluating properties of reconstruction algorithms. The phantom was discretized into a 64x64 image.

Projection data were simulated as follows: we applied the radon transform to the phantom, using 60 angular and 95 radial samples of projections. These projection data were used as a mean rate of a Poisson process. Random samples of projection data were generated according to the above Poisson process.

The application of the wavelet domain EM algorithm is depicted in Figure 2. To compare with, we present in Figures 3 reconstructions of the image obtained by the wavelet domain EM algorithm, applied to the subsets of the approximation coefficients. Figure 4 shows a reconstruction achieved by utilizing prior information on spatial multiresolution structure of the initial image.

In the second part of our experiments we compared performance of the plain EM and CB algorithms with their versions utilizing wavelet domain penalties. In this experiments we used the modified Shepp-Logan phantom (Figure 5) of 128x128. In this phantom an additional hot spot was added. It was used for calculation of the contrast parameter. Examples of reconstructions of the modified Shepp-Logan phantom achieved by plain versions of the EM and the CB algorithms and their wavelet penalty versions (EMWP and CBWP) are given in Figure 6. Clearly, utilizing wavelet domain penalty not only improves quality of reconstruction, arriving at a smoother image, but also provides a better contrast. This fact is quantitatively illustrated in the following two figures. Diagram in Figure 7 depicts comparison of normalized squared errors (NSEs) for plain, postfiltered and wavelet domain penalized versions of EM and CB algorithms. Wavelet domain penalized versions arrive at substantially smaller NSEs. Also, the CB algorithm outperforms the EM in all the cases of comparison but plain versions.

Contrast comparison

There are two parameters which are useful in the contrast calculation: coefficient of variation (CV) and contrast recovery (CR). The CV is defined as the ratio of the standard deviation to the mean-value of the image over some region of interest (ROI). CR for cold lesions in a hot background is calculated as

$$CR_{cold} = 1 - C / H,$$

where C and H are means taken over cold and hot ROI, respectively. For hot lesions in a cold background we compute:

$$CR_{hot} = \frac{H/C-1}{H_{true}/C_{true}-1},$$

where H_{true} / C_{true} is the real ratio of hot lesion to the background in the phantom.

We use the above parameters in order to determine which algorithm provides the best tradeoff between contrast and noise control.

Figure 8 depicts comparison of contrast properties for plain, postfiltered and wavelet domain penalized versions of EM and CB algorithms. In this figure, each point on curves corresponds to the scatter plot of CV versus CR at a particular iteration. Generally speaking, the higher each curve 'climbs', the better is the contrast achieved. The EM algorithm outperforms the CB algorithm slightly in both plain and WT penalty versions, while applying the WT penalty is significantly improves contrast for both EM and CB algorithms.

Figure 9 depicts convergence properties of plain and WT penalty versions of EM and CB algorithms. Wavelet domain penalized versions in both cases converges considerably faster than the plain ones.

6. DISCUSSION

In this work we proposed new algorithms utilizing the WT in the ML PET reconstruction in two different ways. The first way is based on transformation of the parameter space to the wavelet domain and applying an iterative process to the WT coefficients. This strategy provides good results, but computationally not efficient at the moment. The second way is to utilize penalty function defined in the wavelet domain.

The proposed algorithms reveal several desired properties. In particular, the proposed schemes allow estimation of parameters (e.g. the intensity values of 2-D pixels or 3-D voxels in the case of PET) at desired resolutions. In practice, it is desirable to carry out reconstruction on low statistics (i.e. noisy data). Under these circumstances, the maximum likelihood estimate at highest resolution contains high frequency noise even though the original image is known to be relatively smooth. Therefore, a lower resolution reconstruction should be applied to regions with absence of edges. This provides desired regularization, so that a trade-off between increasing resolution and noise suppression is achieved. In contrast, keeping higher resolution components preserves local features in the reconstructed image. This approach is in particular useful in case when *a priori* knowledge on the image structure is available.

Numerical results and comparisons, concerning convergence properties and the quality of reconstruction of the proposed wavelet-based algorithms versus standard algorithms indicate superiority of the proposed method.

The wavelet domain penalty can be applied in two ways: 1) by utilizing some prior knowledge on the spatial and multiresolution structure of the desired image, and 2) by applying penalty function based on the norm of (all) coefficients of the WT representation of the reconstructed image at each iteration. In the second case, using the l_1 norm is of particular interest, since it represents sparse properties of the image. Since most of the medical images are quite sparse, such a penalty can be used without any prior knowledge of the WT representation structure of the desired image.

The current research is concentrated on the comparison of the proposed WT penalty-based method with other penalties used in literature, and on the using the l_1 norm in the penalty function.

7. REFERENCES

[1] A. Dempster, M. Laird, and D. Rubin (1977). Maximum likelihood from incomplete data via the EM algorithm. *Jour. Royal Stat. Soc., 39, no 1, 1-38.*

[2] L. Shepp, Y. Vardi, (1982). Maximum likelihood reconstruction for emission tomography. *IEEE Med. Imaging, 1, 113-122.*

[3] R.M. Lewitt (1992). Alternatives to voxels for image representation in iterative reconstruction algorithms. *Phys. Med. Biol., Vol. 37, No. 3, 705-716.*

[4] F. Jacobs, et al. (1999) A comparative study of 2D reconstruction algorithms using pixels and optimized blobs applied to Fourier rebinned 3D data. *International meeting on fully 3D reconstruction in radiology and nuclear medicine, 43-46.*

[5] Ben-Tal, A. and Nemirovski, A. (1999). "The conjugate barrier method for non-smooth convex optimization", TR #5/99, Oct. 1999, Minerva Optimization Center, Technion.

[6] Margalit, T, et al. (1999). "The ordered sets mirror descent and conjugate barrier optimization algorithms adapted to the 3D PET reconstruction problem", TR #7/99, Nov. 1999, Minerva Optimization Center, Technion.

[7] Nemirovsky, A. Personal communications.

[8] J. A. Fessler, N. H. Clinthorne, W. L. Rogers. "Regularized emission image reconstruction using imperfect side information". Proc. IEEE Nuc. Sci. Symp. Med. Im. Conf., vol. 3, pp. 1991-1995, 1991.

[9] D. F. Yu, J. A. Fessler. "Three-dimensional non-local edge-preserving regularization for PET transmission reconstruction". Proc. IEEE Nuc. Sci. Symp. Med. Im. Conf., 2000. To appear. (oral)

Acknowledgement

This research has been supported by the Ollendorff Minerva Center and by the Technion V.P.R. Fund for the promotion of sponsored research – The Goldberg Fund (050-011).

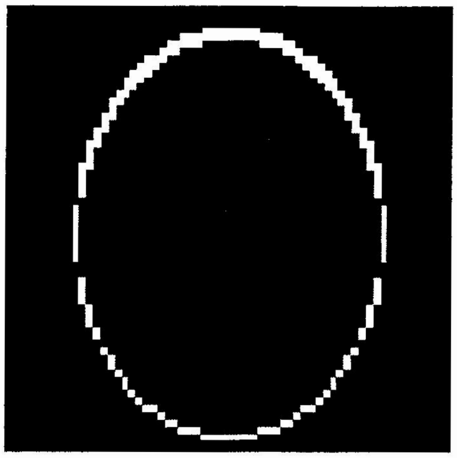

Figure 1. Shepp-Logan phantom

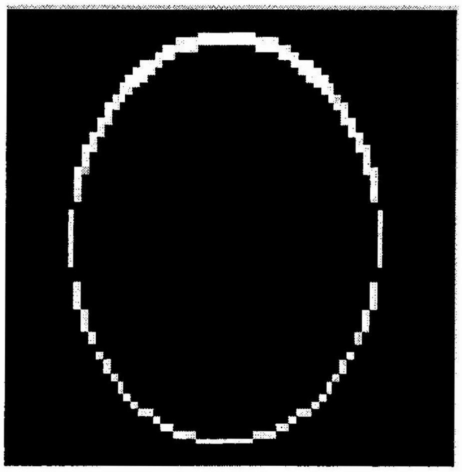

Figure 2. Image reconstructed from the finest scale, using all the scales, of the wavelet domain EM.

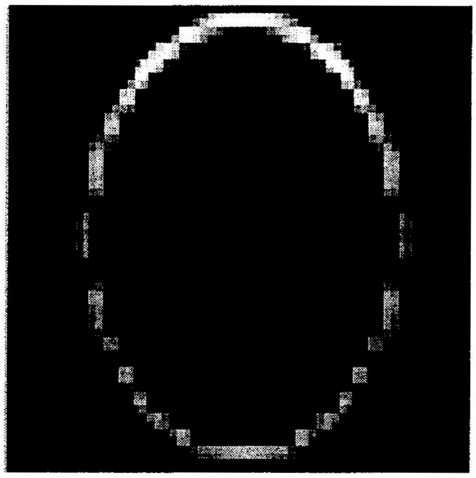

Figure 3. The wavelet domain EM, applied to the subset of the approximation coefficients.

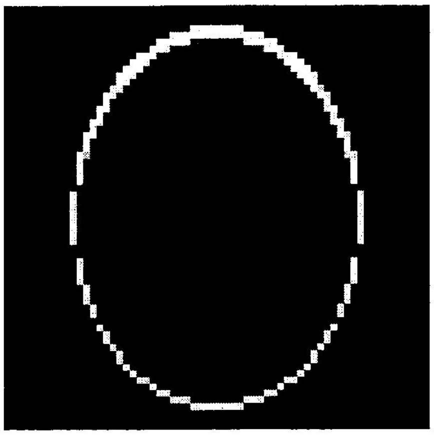

Figure 4. Regularized reconstruction achieved by utilizing prior information

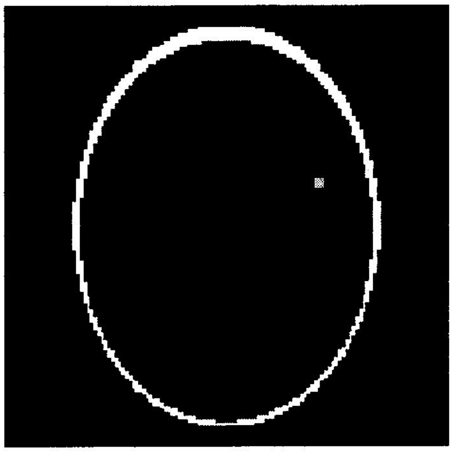

Figure 5. Modified Shepp-Logan phantom

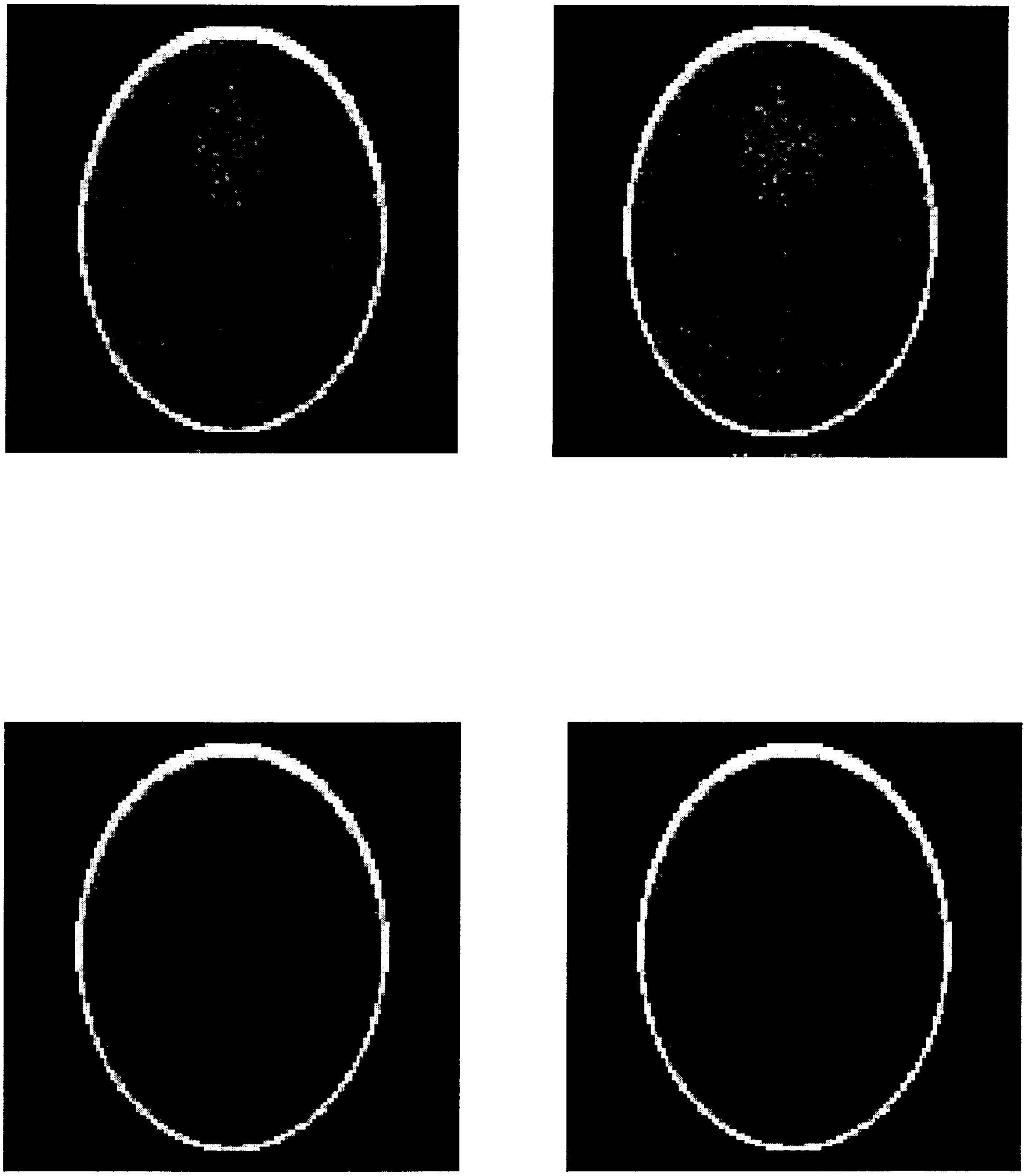

Figure 6. Comparison of the modified Shepp-Logan phantom reconstruction: EM reconstruction (upper left); CB reconstruction (upper right); EM with wavelet penalty reconstruction (lower left); CB with wavelet penalty reconstruction (lower right).

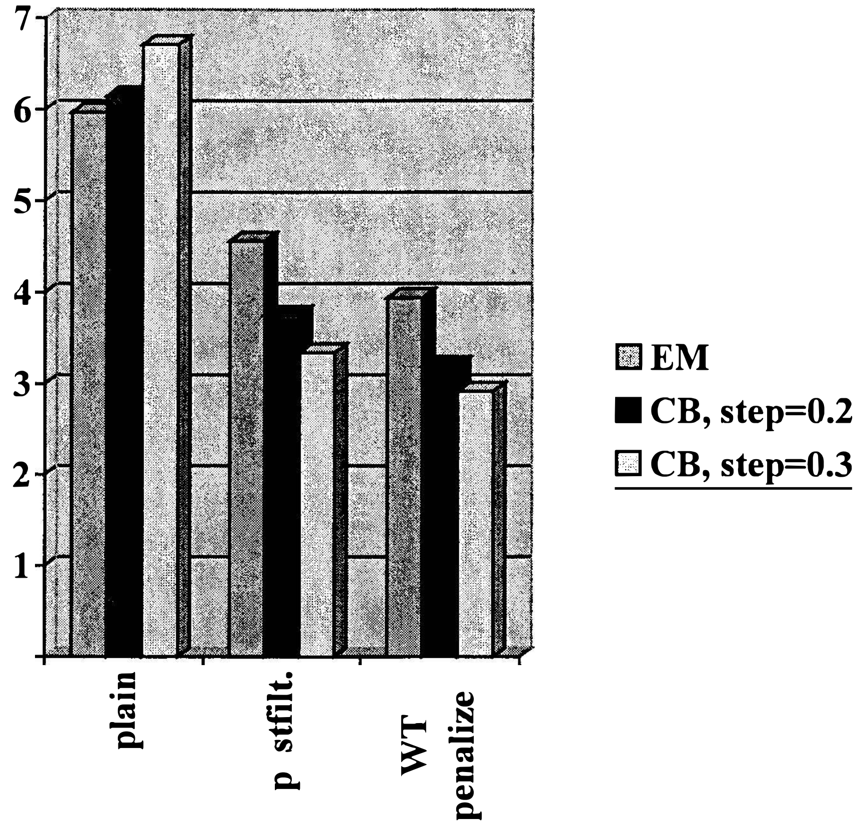

Figure 7. Comparison of normalized squared reconstruction errors.

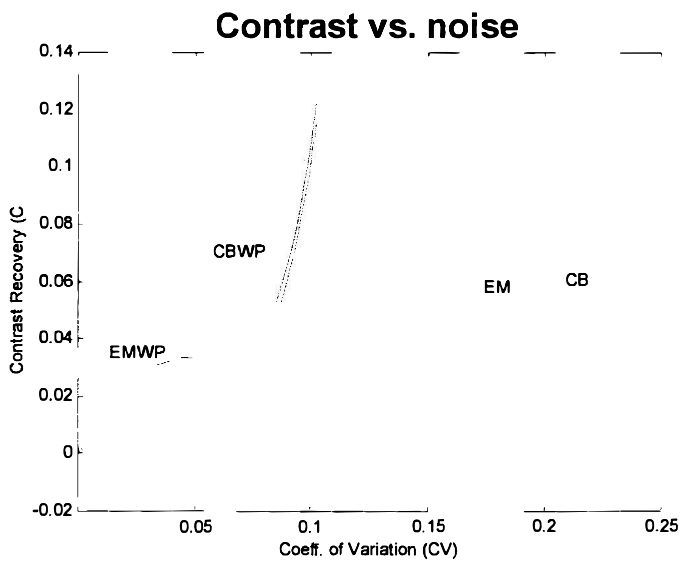

Figure 8. Comparison of contrast parameter at each iteration for plain and WT penalty versions of EM and CB algorithms

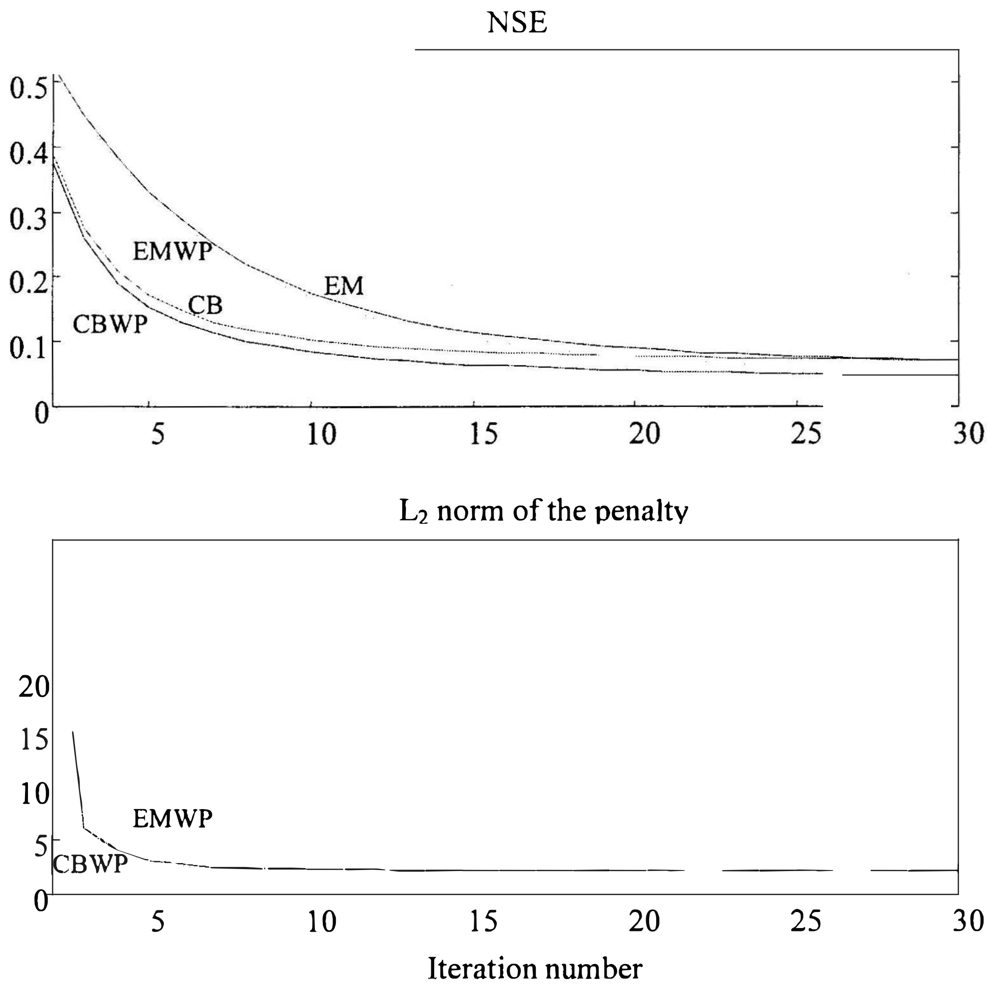

Figure 9. Convergence properties of EM and CB algorithms.

Appendix
Wavelet based multiresolution decomposition and wavelet packets

The following brief outline of the pyramidal algorithm for multiresolution analysis is based on the formalism of Mallat [16]. The algorithm is given here for one-dimensional functions and can be defined in a similar way for the dyadic, separable two dimensions, in which case, one obtains a 4-band pyramid or tree (see below). (One can also obtain a 2-band pyramid by using a quinc sampling scheme and two-dimensional nonseparable wavelets [17]).

The multiresolution framework is based on two sets of subspaces of $L^2(R)$ - V_j and $W_j, j \in Z$, which satisfy the following conditions:

1) $\ldots V_{-1} \supset V_0 \supset V_1 \ldots$
2) $W_j \cap W_k = \emptyset; \forall j \neq k \in Z$
3) $V_j \cap W_j = \emptyset$
4) $V_j \cup W_j = V_{j+1}; \forall j \in Z$

In addition, V_j is dense in $L^2(R)$ for $j \to \infty$. Index j is a scale parameter, and the scale becomes finer (i.e., the resolution increases) with increasing j.

The projection of a function $f(t)$ onto subspace V_j is an approximation of $f(t)$ at scale j, and the projection of the function $f(t)$ onto subspace W_j provides the detail of $f(t)$ at scale j. The detail function contains the information that is lost in the transition from $A_j f(t)$ to $A_{j+1} f(t)$.

Starting from a single function $\phi(t)$, the father wavelet, it is possible to generate an orthonormal basis of the scaling functions $\phi_{jk}(t) = 2^{j/2}\phi(2^j t - k), j, k \in Z$, spanning V_j. Similarly, starting from a single function $\psi(t)$, the mother wavelet, one can obtain an orthonormal basis of wavelet functions $\psi_{jk}(t) = 2^{j/2}\psi(2^j t - k)$, spanning W_j, where k is a shift parameter.

Thus the approximation and detail of the function at scale j are represented by

$$A_j f(t) = \sum_{k \in Z} a_j(k)\phi_{jk}(t), \tag{1A}$$

$$D_j f(t) = \sum_{k \in Z} d_j(k)\psi_{jk}(t), \tag{2A}$$

where

$$a_j(k) = < f(t), \phi_{jk}(t) >, \tag{3A}$$

$$d_j(k) = < f(t), \psi_{jk}((t) > \tag{4A}$$

Since the subspaces V_j and W_j are orthonormal, a unique inverse transform exists.

A multi-level analysis representation of such a sampled function in terms of its details and approximation functions up to some reference level J is given by:

$$f(t) = A_J f(t) + \sum_{j \geq J} D_j f(t). \tag{5A}$$

Further, let the sequences h and g, describing a lowpass and a highpass filters, respectively, satisfy the following relationships, the so-called refinement equations:

$$\phi(t) = \sum_{k \in Z} \sqrt{2}\, h(k)\phi(2t - k), \tag{6A}$$

$$\psi(t) = \sum_{k \in Z} \sqrt{2}\, g(k)\phi(2t - k). \tag{7A}$$

The approximation and detail coefficients at scale j, a_j and d_j, respectively, can be recursively calculated from the approximation coefficients a_{j+1} at a finer scale, by convolving it with filters $h(k)$ and $g(k)$, followed by a dyadic down-sampling, i.e.

$$a_j(k) = h * a_{j+1}(2k), \tag{8A}$$

$$d_j(k) = g * a_{j+1}(2k), \tag{9A}$$

where * denotes a convolution operation. The next step in a multi-level decomposition splits the approximation coefficients a_j using the same operations, producing recursively the coefficients a_{j-1} and d_{j-1}.

Let s be a vector containing L samples of a continuous function $f(t)$, and let L be a power of 2. In this case, we can consider these samples as approximation coefficients of $f(t)$ at the finest (available) scale $J = \log_2 L$, and a multi-level wavelet analysis of a sampled signal s can be rewritten in the matrix form:

$$c = Ws, \tag{10A}$$

where a new features vector in the wavelet domain has the following coefficients structure: $c = [a_0, d_0, d_1, ..., d_{J-1}]^T$, and W is a matrix of an orthonormal wavelet basis, describing the multiresolution decomposition given in (8A) and (9A). The corresponding tree structure of coefficients for the case of a 3-level decomposition is depicted in Figure 1A.

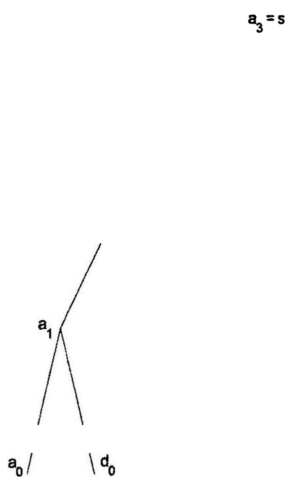

Figure 1A. Multiresolution wavelet

The complement operations of those given in (8A) and (9A), i.e. the calculation of a finer scale approximation coefficients a_{j+1} from a coarser scale approximation and detail coefficients a_j and d_j, is performed by a dyadic upsampling followed by the corresponding convolutions with filters $h(k)$ and $g(k)$

$$a_{j+1}(k) = \sum_{m \in Z} h(2m - k)a_j(k) + \sum_{m \in Z} g(2m - k)d_j(k). \tag{11A}$$

A corresponding multi-level wavelet synthesis of a sampled signal s from its wavelet coefficients can be written in the matrix form as:

$$s = W^T c. \tag{12A}$$

Let us define the following sequence of functions $\varphi_n(t)$, $n \in N$ so that

$$\varphi_{2n}(t) = \sum_{k \in Z} \sqrt{2}\, h(k)\varphi_n(2t - k), \tag{13A}$$

$$\varphi_{2n+1}(t) = \sum_{k \in Z} \sqrt{2}\, g(k)\varphi_n(2t - k), \tag{14A}$$

where $\varphi_0(t) = \phi(t)$, and $\varphi_1(t) = \psi(t)$. Thus, starting from the family of generating functions $\varphi_n(t)$, $n \in N$, and constructing from them orthogonal wavelet waveforms, we arrive at the triple-indexed family of functions:

$$\varphi_{jnk}(t) = 2^{j/2}\varphi_n(2^j t - k), \; j,k \in Z, n \in N. \tag{15A}$$

As before, j,k are the scale and shift parameters, respectively, and n is an explicit frequency parameter, related to the number of oscillations of a particular generating function $\varphi_n(t)$. The set of functions $\varphi_{jn}(t)$ forms a (j,n) wavelet packet. This set of functions can be split into two parts at a coarser scale: $\varphi_{j-1,2n}(t)$ and $\varphi_{j-1,2n+1}(t)$. It follows that these two form an orthonormal basis of the space which is spanned by $\varphi_{jn}(t)$. Thus, we arrive at a family of wavelet packet functions on a binary tree (Figure 2A). The nodes of this tree are numbered by two indices: the depth of the level $j = 0, 1, .., J$, and the number of node $n = 0, 1, 2, 3, ..., 2^j\!-\!1$ at the specified level.

Using such a family of functions allows one to analyze given signals not only with a scale-oriented decomposition but also with reference to frequency subbands. There are 2^L wavelet bases in such a library (L is the number of samples in the signal), and, therefore, 2^L ways to represent a given signal. Naturally, the library contains the wavelet basis. There are several criteria for choosing the best basis, i.e. the best tree, for a given signal (see, [18] for a survey).

The *Center for Communication and Information Technologies* (CCIT)

is managed by the Department of Electrical Engineering.

This Technical Report is listed also as

EE PUB #1271, January 2001.